BRIEF COMMUNICATION

Novel features of early burst suppression predict outcome after birth asphyxia

Kartik K. Iyer[1,2], James A. Roberts[1], Marjo Metsäranta[3], Simon Finnigan[4], Michael Breakspear[1,5,6] & Sampsa Vanhatalo[7,8,]

[1]Systems Neuroscience Group, QIMR Berghofer Medical Research Institute, Brisbane, Queensland, Australia
[2]School of Medicine, Faculty of Medicine and Biomedical Sciences, University of Queensland, Queensland, Australia
[3]Children's Hospital, Helsinki University Central Hospital and University of Helsinki, PO Box 281, Helsinki, HUS, 00029, Finland
[4]The University of Queensland Centre for Clinical Research (UQCCR) and Perinatal Research Centre, Brisbane, Queensland, Australia
[5]School of Psychiatry, University of New South Wales and The Black Dog Institute, Sydney, New South Wales, Australia
[6]The Royal Brisbane and Woman's Hospital, Brisbane, Queensland, Australia
[7]Department of Children's Clinical Neurophysiology, Helsinki University Central Hospital, PO Box 280, Helsinki, HUS, 00029, Finland
[8]Department of Neurological Sciences, University of Helsinki, Helsinki, 00014, Finland

Correspondence

Sampsa Vanhatalo, Department of Children's Clinical Neurophysiology, Helsinki University Central Hospital, PO Box 280, Helsinki, HUS 00029, Finland. Tel: +358-50-528 6119; Fax: +358-9-4711; E-mail: sampsa.vanhatalo@helsinki.fi

Abstract

Burst suppression patterns in the electroencephalogram are a reliable marker of recent severe brain insult. Here we analyze statistical properties of bursts occurring in 20 electroencephalographic recordings acquired from hypothermic asphyxic newborns in the hours immediately following birth. We show that the distributions of burst area and duration in these acute data predict later clinical outcome in both structural neuroimaging and neurodevelopment. Our findings indicate the first early electroencephalographic metrics that offer outcome prediction in asphyxic neonates undergoing hypothermia treatment.

Introduction

Hypoxic ischemic encephalopathy (HIE) following perinatal asphyxia is the leading cause of acquired, severe neurodevelopmental disability.[1] The neurodevelopmental outcome of HIE depends on how quickly neuronal function recovers from the asphyxic insult. Continuous electroencephalography (EEG) monitoring has become a widely accepted practice in neonatal intensive care units (NICUs).[2–4] A key EEG hallmark of severely injured brain function is a pattern of low amplitude (suppressed) EEG punctuated by irregular high amplitude bursts (Fig. 1A) known as burst suppression (BS).[5] Several studies have shown that the resolution of BS in EEG recordings within 6–12 h of birth correlates strongly with a favorable neurodevelopmental outcome.[4,6] Identification of BS and its recovery time in asphyxic newborns has thus been used as a prognostic indicator of brain function to guide therapeutic decisions. While clinical decisions to commence therapeutic hypothermia after birth asphyxia are often based on observing BS in the early EEG, hypothermia treatment itself was recently found to significantly delay BS recovery, hence compromising the utility of early EEG in outcome prediction[7,8] (see also Ref. 9).

The observation of BS in EEG recordings has long been identified as indicating acute neuronal compromise.[1,10–12] Neurophysiological interpretation of BS conventionally rests upon a dichotomous presence-versus-absence classification.

While qualitative assessment of "burst sparseness" – a low overall frequency of bursts – may be taken as an additional sign of severity,[12] no properties of the bursts themselves have been shown to provide useful prognostic indicators. Exploiting recent advances in complex systems analysis,[13–16] we sought to characterize statistical properties of BS, in particular features related to burst duration (BD) and area (i.e., burst size). These features of BS carry novel, clinically important information neither provided by current brain monitoring paradigms nor evident by visual inspection of EEG alone. Our findings provide a novel approach for predicting outcome, based on identifying information embedded in BS activity early after brain injury, a task that has proven thus far elusive.

Patients and Methods

We studied EEG recordings of 20 consecutively admitted newborns (gestational age 39 ± 2 weeks) monitored due to HIE following perinatal asphyxia at the tertiary level NICU of Helsinki University Central Hospital. HIE was assessed according to conventional criteria,[17] including lethargy, stupor, or coma, with one or more findings of hypotonia, abnormal reflexes or clinical seizures. The EEG was acquired from biparietal electrodes at 250 Hz using a NicOne or Olympic EEG device (Cardinal Healthcare, Nicolet Biomedical, Madison, WI and Natus Medical, San Carlos, CA). Lengthy epochs of BS that were relatively artifact-free (120 ± 90 min, range 30–600 min) were filtered at 1–20 Hz and further analyzed with custom software in Matlab (Mathworks, Natick, MA). BS was determined visually as an EEG pattern consisting of activity bursts (mixture of sharp, slow waves) periodically interrupted by multiple episodes of suppressed cortical activity ($\sim$<10 μV). Although BS somewhat resembles trace alternant and trace discontinue activity patterns, these are distinct phenomena. First, they are part of the pseudo-periodic vigilance state cycling that is absent early after asphyxia.[3,7] Second, they only occur in younger preterm babies (trace discontinue), or their suppression period is insufficiently suppressed for classification as BS (trace alternant). Cooling onset preceded EEG recordings in all babies (see Table S1). Clinical data collated from patient reports included: reports from magnetic resonance imaging (MRI) scans during the first week after birth; birth details; NICU drug treatments; and outcome description from the last visit to routine neonatal outpatient clinic (age 12–39 months). Patients were divided into two categories based on MRI findings (presence/absence of a thalamic lesion), and further into four categories based on clinical outcomes: normal versus mildly, moderately, and severely abnormal (see Table S1 for full details). Four of the 20 available neonatal data were excluded from further analyses due to the presence of excessive seizure activity ($n = 1$), early adminis-

tration of sedative drugs that likely affected BS ($n = 1$), or missing reliable clinical or MRI information ($n = 2$). The use of patient data for this study was approved by the Ethics Committee of the Hospital for Children and Adolescents, Helsinki University Central Hospital.

To extract statistical properties of the bursts, we first developed an adaptive thresholding method to detect the occurrence of bursts in the EEG (Fig. 1, and see Fig. S1 for preprocessing steps). We then extracted three burst metrics for each infant: (1) mean BD and its coefficient of variation (CV), (2) scaling exponent (α) of the cumulative distribution function (CDF)[18] of the burst areas (BA) in each recording (Fig. 1E), and (3) slope value based on the relationship between BD and BA (Fig. 1F). Here, the scaling exponent (α) captures how quickly the number of bursts diminishes as a function of increasing area: A large exponent ($\alpha \gg 1.5$) indicates that most bursts are very small in area, whereas the converse ($\alpha \sim 1.5$) indicates that larger bursts occur relatively more often. Since the distribution closely follows a truncated power law, there is no single characteristic size but rather a broad "scale-free" regime, limited only by finite brain capacity. Our novel metrics focus on properties of bursts, specifically the heterogeneity of BAs, as well as the relationship between BAs and BDs. In addition, we benchmarked these novel measures against those established in prior research, namely the mean and CV of interburst interval (IBI) durations.[10] The slope values from BA versus BD plots and BA CDF plots were extracted as described in Figure 1E and F. Notably, the members in our team scripting and running the analysis algorithms did not perform visual EEG interpretation nor clinical data collection.

Group comparisons were conducted using one-way analysis of variance (ANOVA) and verified with nonparametric Mann–Whitney U tests. Correlations of clinical outcomes to EEG metrics were measured using Spearman's rank correlation coefficient.

Results

Visual inspection of bursts occurring during post asphyxic EEG characteristically showed erratic and irregular fluctuations of BS in the amplitude trace (Fig. 1A), as well as the corresponding power trace (Fig. 1B and C). We hence examined the variability in BA by plotting its CDF (Fig. 1E) and the relationship between BA and BD (Fig. 1F). We first observed that the CDFs of BA show a robust, linear scaling relationship over several orders of magnitude (Fig. 1E). We also observed a robust power-law relationship between BA and BD over four orders of magnitude (Fig. 1F). Comparison with subsequent MRI findings (Fig. 2A and B) showed that α was significantly higher ($F_{1,16} = 5.39$, $P = 0.035$), and the slope between BAs versus BDs was significantly higher ($F_{1,16} = 7.89$, $P = 0.013$) in babies with thalamic
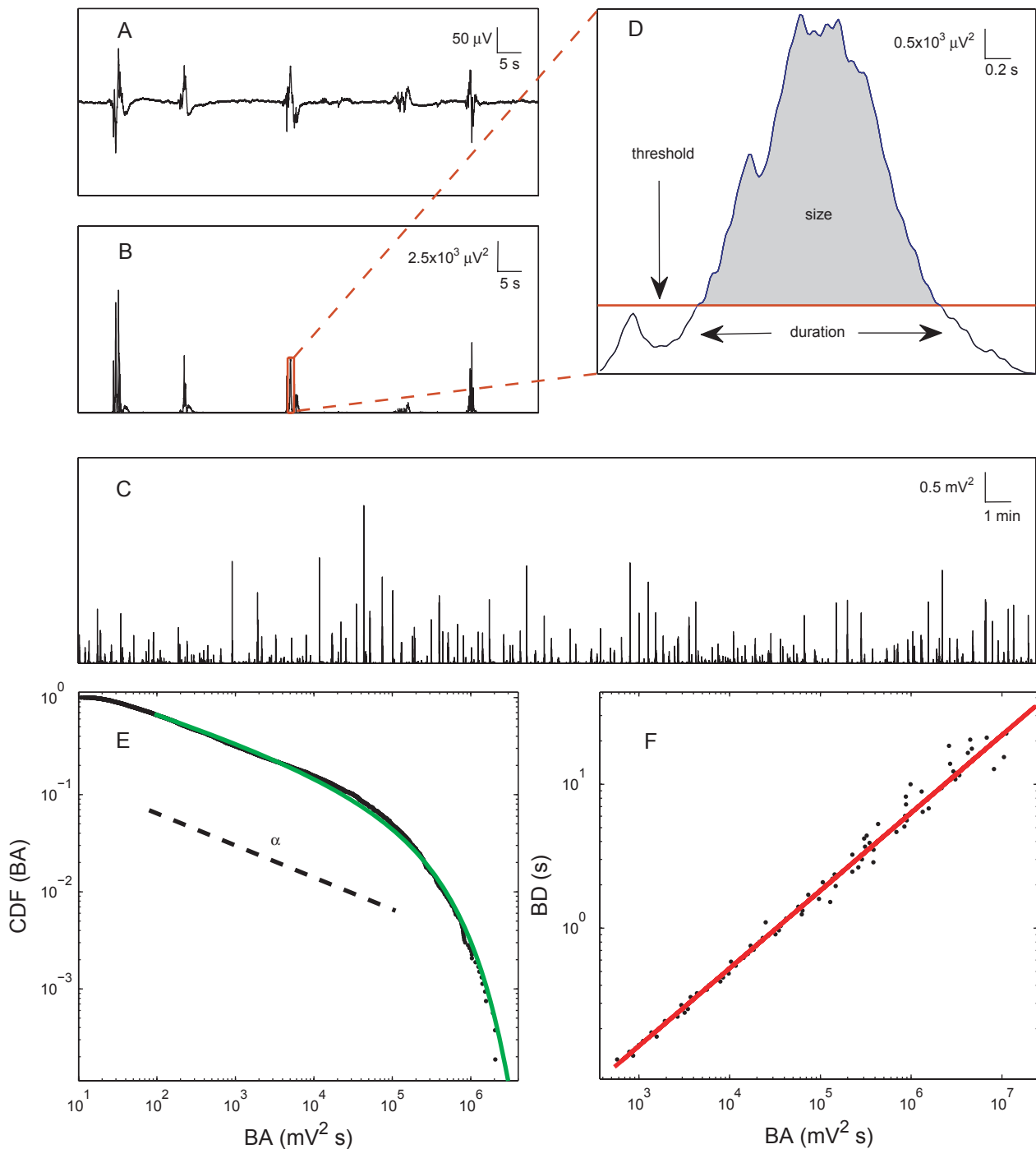
Figure 1. Extraction of burst suppression metrics. (A) Example EEG epoch with burst suppression pattern (P3–P4 derivation). (B) Instantaneous power (amplitude-squared) of the same EEG epoch obtained from the amplitude envelope (via Hilbert transform). (C) Instantaneous power over 80 min of a recording to illustrate the variability in the size of bursts over time. (D) Sample burst taken from graph (B) to illustrate the burst measures. The automated threshold was used for defining the burst area (BA) and the burst duration (BD). (E) Upper cumulative distribution function (CDF) of BA in one infant shows that it follows an exponentially truncated power law distribution (fit shown in green) over several orders of magnitude. On the basis of these observations (refer to methods[14,16,17]), we extracted the scaling exponent (α) of the distribution. Here the dashed line illustrates the corresponding α for the BA as given by the CDF. (F) Relationship between BAs and BDs in one infant, plotted in double logarithmic coordinates. Points are median durations and median areas calculated after dividing the data into 250 logarithmic bins, with the robust linear relationship quantified by the slope of the linear least-squares fit (red line).
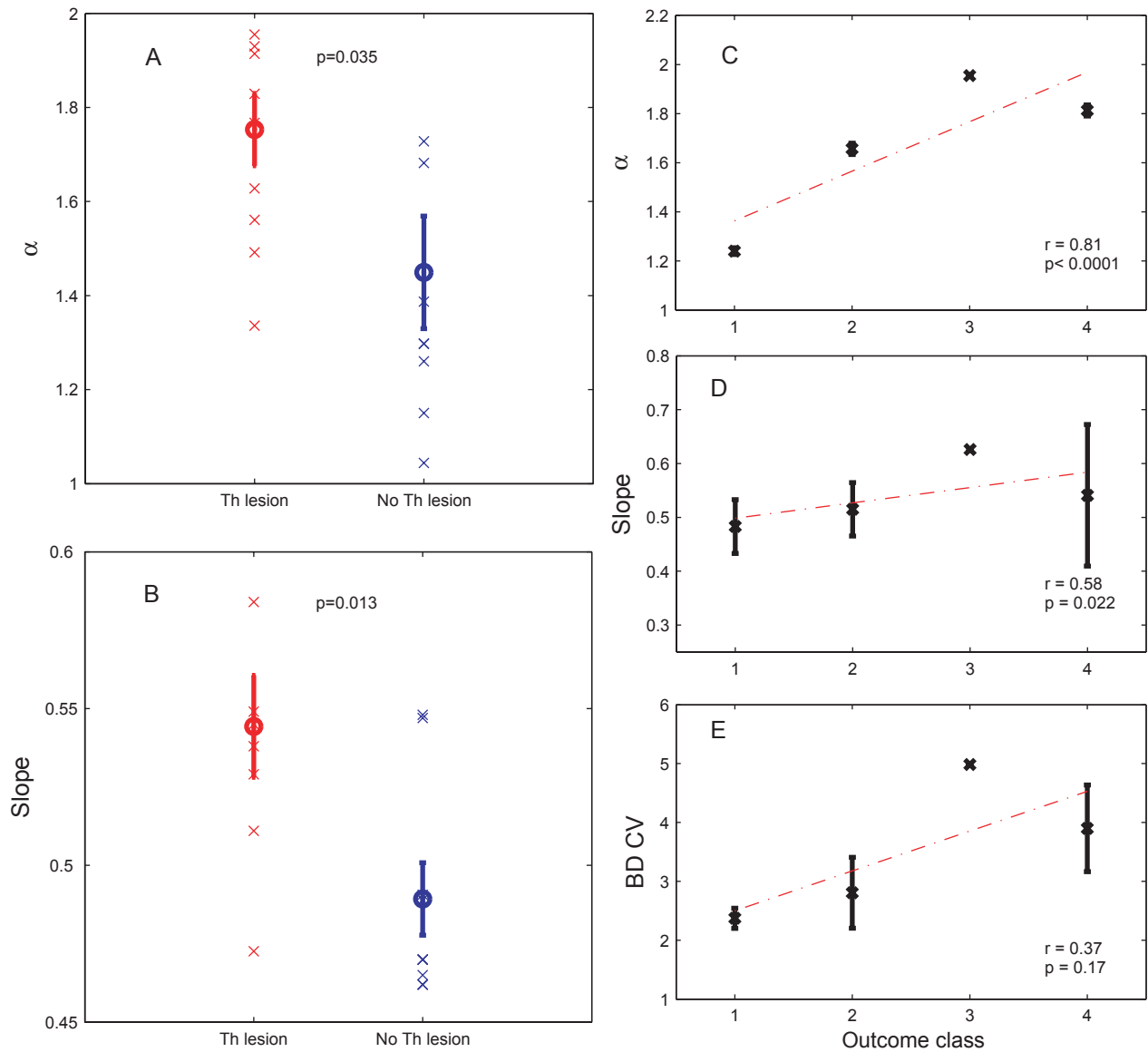
Figure 2. Prediction of outcome with early burst suppression metrics. (A and B) Comparison of burst suppression metrics during first hours after birth to subsequent MRI changes observed several days later. Infants who developed thalamic lesion (Th lesion) apparent in MRI had significantly higher exponents α (A) in the BAs, and a significantly higher slope values (B) in the relationship between BA and BD. The graphs show mean $\pm$ SEM (circles and lines) and the individual data points (crosses). (C–E) Comparison of burst suppression metrics during first hours after birth to clinical outcome categories later in infancy (1 = normal; 2 = mildly abnormal; 3 = moderately abnormal; 4 = severely abnormal; see also Table S1). There was a statistically significant correlation between clinical outcome and (C) α (D) slope and a positive correlation in (E) BD CV. Significant group differences were also found when dividing outcomes into two categories, good (1 and 2) and poor (3 and 4).

lesions. Moreover, both of these metrics showed a significant correlation with neurodevelopmental outcome ($r = 0.81$, $P < 0.0001$, and $r = 0.58$, $P = 0.022$, respectively; Fig. 2D and E). Visual comparison of different outcome groups shows considerable variability over time and between records, due to both temporal evolution of BS patterns and physical factors (e.g., subcutaneous swelling). Two extreme cases (normal MRI and outcome versus abnormal MRI and outcome) are shown in Figure S4, emphasizing the need for objective, statistically sound methods for their interpretation.

We then benchmarked these findings against conventional measures of bursts (BDs, BD CVs), and their intervals (IBIs). Statistical analyses revealed that BD CV was significantly higher ($F_{1, 16} = 4.92$, $P = 0.042$) in babies with thalamic lesions compared to those with normal

MRI findings. However, no difference was found in the mean duration of bursts ($F_{1,16} = 0.17$, $P = 0.68$) or the mean IBIs ($F_{1,16} = 0.05$, $P = 0.81$). In addition, BD CV showed a positive correlation with the developmental outcome ($r = 0.37$, $P = 0.17$; Fig. 2C). No correlation was seen between mean BD and any measure of IBIs.

Discussion

Our findings show that novel burst statistics derived objectively from EEG soon after perinatal asphyxia correlate significantly with MRI findings obtained only several days later, as well as with neurodevelopmental outcomes obtained later in infancy. The measures of burst areas and durations, and their interrelationships, were derived from routinely collected EEG records in cooled asphyxic newborns where traditional measures of IBIs or resolution of BS have insufficient prognostic reliability.[6,7] The present observations have both theoretical and practical implications.

Theoretically, the presence of robust scale-free statistics is compatible with the notion that a severely compromised brain operates in a critical balance between excitation and inhibition. While such properties of cortical dynamics cannot be assessed using traditional EEG measures, they are rapidly extracted with novel and robust mathematical tools recently developed in computational neuroscience and physics.[14,18,19] Pragmatically, extracting clinically informative statistics from a very large number of bursts engenders such metrics insensitive to common noise-related confounders. Moreover, our observations significantly challenge the clinical practice of perceiving BS as a uniform entity.[12] Rather, the present findings are compatible with the alternative notion that functional brain recovery is already ongoing during BS where it can be assessed from the statistical characteristics of cortical bursting rather than from the traditionally measured lengths of inactive (IBI) periods.

Practically, our measures present several clinical advantages. First, because they focus on the bursts only, they avoid a need for uninterrupted recordings. Hence, these measures are robust to intermittent artifacts present in the electrically noisy NICU environment and challenge traditional analyses of EEG monitoring. Second, our EEG-derived measures provide outcome predictions 4–7 days earlier than MRI findings, possibly enabling early guidance of individually targeted therapeutic decisions. Third, our paradigm is data-driven, reducing interindividual variability in the overall level of EEG amplitudes caused by technical variations (e.g., interelectrode distance, constant artifact, or subcutaneous swelling). Amplitude variance caused by artifacts is a serious confounder prevalent in many existing approaches, particularly ampli-

tude-integrated EEG (aEEG, a.k.a. Cerebral Function Monitor [CFM][20]). The data-driven algorithm employs burst detection via an adaptive threshold, where scaling properties reported were reliable over a range of thresholds (see Supplementary Material). Notably, the EEG measures introduced here are designed for rapid automated prognostication, and thus could be readily implemented as software features in currently used brain monitoring systems.

While our findings are encouraging, the dataset presently studied has limitations, such as a limited sample size and outcome classifications that were retrospectively extracted from clinical archives instead of prospectively collected standardized neurodevelopmental tests. Future studies on larger patient series with standardized outcome measures are needed to validate the present observations. It will also be important to examine the clinical potential of our measures in differential diagnosis of BS etiologies (e.g., asphyxia, trauma, sedative drugs), a common diagnostic challenge in acute patient care. Finally, it is likely that these same statistical properties of BS are also found in adult neuro-intensive care, expanding the clinical implications of our findings.

Acknowledgments

Conflict of Interest

None declared.

References

1. Bonifacio SL, Glass HC, Peloquin S, Ferriero DM. A new neurological focus in neonatal intensive care. Nat Rev Neurol 2011;7:485–494.

2. Nash K, Bonifacio S, Glass H, et al. Video-EEG monitoring in newborns with hypoxic-ischemic encephalopathy treated with hypothermia. Neurology 2011;76:556–562.

3. Hellström-Westas L, Rosén I, eds. Continuous brain-function monitoring: state of the art in clinical practice. Semin Fetal Neonatal Med. 2006; 11:503–511.

4. van Rooij LG, Toet MC, Osredkar D, et al. Recovery of amplitude integrated electroencephalographic background patterns within 24 hours of perinatal asphyxia. Arch Dis Child Fetal Neonatal Ed 2005;90:F245–FF251.

5. Holmes G, Rowe J, Hafford J, et al. Prognostic value of the electroencephalogram in neonatal asphyxia. Electroencephalogr Clin Neurophysiol 1982;53:60–72.

6. Toet M, Hellström-Westas L, Groenendaal F, et al. Amplitude integrated EEG 3 and 6 hours after birth in full term neonates with hypoxic–ischaemic encephalopathy. Arch Dis Child Fetal Neonatal Ed 1999;81:F19–F23.

7. Thoresen M, Hellström-Westas L, Liu X, de Vries LS. Effect of hypothermia on amplitude-integrated electroencephalogram in infants with asphyxia. Pediatrics 2010;126:e131–e139.

8. Hallberg B, Grossmann K, Bartocci M, Blennow M. The prognostic value of early aEEG in asphyxiated infants undergoing systemic hypothermia treatment. Acta Paediatr 2010;99:531–536.

9. Kessler SK, Topjian AA, Gutierrez-Colina AM, et al. Short-term outcome prediction by electroencephalographic features in children treated with therapeutic hypothermia after cardiac arrest. Neurocrit Care 2011;14:37–43.

10. Grigg-Damberger MM, Coker SB, Halsey CL, Anderson CL. Neonatal burst suppression: its developmental significance. Pediatr Neurol 1989;5:84–92.

11. Niedermeyer E, Sherman DL, Geocadin RJ, et al. The burst-suppression electroencephalogram. Clin Electroencephalogr 1999;30:99.

12. Walsh B, Murray D, Boylan G. The use of conventional EEG for the assessment of hypoxic ischaemic encephalopathy in the newborn: a review. Clin Neurophysiol 2011;122:1284–1294.

13. Spasojević D, Bukvić S, Milošević S, Stanley HE. Barkhausen noise: elementary signals, power laws, and scaling relations. Phys Rev E 1996;54:2531.

14. Sethna JP, Dahmen KA, Myers CR. Crackling noise. Nature 2001;410:242–250.

15. Beggs JM, Plenz D. Neuronal avalanches in neocortical circuits. J Neurosci 2003;23:11167–11177.

16. Friedman N, Ito S, Brinkman BA, et al. Universal critical dynamics in high resolution neuronal avalanche data. Phys Rev Lett 2012;108:208102.

17. Sarnat HB, Sarnat MS. Neonatal encephalopathy following fetal distress: a clinical and electroencephalographic study. Arch Neurol 1976;33:696–705.

18. Clauset A, Shalizi CR, Newman ME. Power-law distributions in empirical data. SIAM Rev 2009;51:661–703.

19. Shew WL, Yang H, Petermann T, et al. Neuronal avalanches imply maximum dynamic range in cortical networks at criticality. J Neurosci 2009;29:15595–15600.

20. Hellström-Westas L, de Vries, LS, Rosén I. An atlas of amplitude-integrated EEGs in the newborn. 2nd ed. London: Taylor & Francis, 2008.

Supporting Information

Additional Supporting Information may be found in the online version of this article:

Figure S1. This example EEG (P3–P4 derivation) demonstrates how the instantaneous EEG amplitude (red; amplitude at each time point) was computed using the Hilbert transform, a well-established method. The instantaneous power was then computed from the amplitude by taking its square at each time sample (see Fig. 1C).

Figure S2. In order to maximize objectivity in our analysis, we developed a burst detection algorithm that automatically identifies a threshold for each recording. A burst is defined as a series of consecutive time points beginning where the signal crosses above threshold and ending where the signal next crosses below threshold. The thresholding algorithm involves scanning through a wide range of thresholds (x axis) and counting the number of bursts for each threshold (y axis). The identified threshold is that which yields the most bursts (red circle). This procedure overcomes the proven ambiguity in visual burst detection[1] as it yields reproducible and mathematically unambiguous bursts. Inset: example instantaneous power signal (black) and its identified threshold (red).

Figure S3. Four additional examples of infant recordings showing reliability of our automated adaptive thresholding algorithm. In each case (and this was the case for all datasets) the relationship between threshold and the number of bursts follows the same unimodal form yielding one threshold value (red circles) that maximizes the number of bursts detected.

Figure S4. These EEG examples show 45-sec epochs of BS recordings in two babies that had either normal (above) or abnormal (lower) outcomes. In our overall dataset we observe that burst events span a wide range of durations, with a substantial number of long bursts with durations longer than 2 sec (the 16 babies in our outcome groups yielded an average of 236 long bursts each).

Table S1. Clinical details and further information about the EEG recordings of 20 infants.